PHYSICAL REVIEW B VOLUME 50, NUMBER 2 1 JULY 1994-II

Small-angle scattering by fractal aggregates: A numerical investigation of the crossover between the fractal regime and the Porod regime

Anwar Hasmy, René Vacher, and Rémi Jullien
Laboratoire de Science des Matériaux Vitreux, Université Montpellier II, Place Eugène Bataillon, 34095 Montpellier Cedex 5, France
(Received 11 April 1994)

Fractal aggregates are considered computationally using off-lattice cluster-cluster aggregation models. The aggregates are made of spherical particles of different sizes distributed according to a Gaussian-like distribution characterized by a mean a_0 and a standard deviation σ. The wave-vector-dependent scattered intensity $I(q)$ is computed in order to study the influence of the particle polydispersity on the crossover between the fractal regime and the Porod regime. It is shown that, given a_0, the location q_c of the crossover decreases as σ increases. The dependence of q_c on σ can be understood from the evolution of the shape of the center-to-center interparticle-distance distribution function.

Small-angle x-ray scattering as well as small-angle neutron scattering have been widely used to study the structure of disordered systems.[1–8] In particular they have allowed one to demonstrate that silica aerogels are made of connected fractal "blobs."[3,4] In such materials, the wave-vector-dependent scattered intensity $I(q)$ exhibits two crossovers related to the two characteristic lengths, mean particle diameter a_0 and mean blob size ξ. The first one separates the low-q ($q \ll \xi^{-1}$) saturation, called the Guinier regime,[9] from the intermediate power-law behavior,[3,4] called the fractal regime. The second one, on which we will focus in this paper, separates the fractal regime from the high-q ($q \gg a_0^{-1}$) q^{-4} behavior, called the Porod regime.[9]

In some previous studies, it was assumed that the crossover between the fractal regime and the Porod regime was always exactly located at $q_c = 2\pi/a_0$. This assumption was even used by some authors to quantitatively determine the average diameter[5,6] or the gyration radius[4,7] of the particles. In several other papers, an average particle radius was extracted from a fit of the scattered intensity $I(q)$ to analytical expressions which do not include polydispersity.[2,8] Such kind of analysis has been done in the case of base catalyzed and neutrally reacted silica aerogels where the particle size polydispersity impedes the determination of a_0 by conventional methods such as electron micrography. In this paper we show that such an assumption is only valid when the standard deviation σ of the particle size is small compared to the average a_0 .

In previous papers[10,11] it has been shown that cluster-cluster aggregation models[12] can satisfactorily reproduce the structure of aerogels. Furthermore, if we are only interested in short-range correlations, it is sufficient to consider a single aggregate obtained with a simplified aggregation process: the hierarchical cluster-cluster model.[13]

Here for simplicity we have considered the case of chemically limited cluster-cluster aggregation (CLCA) (Ref. 14) using a three-dimensional off-lattice hierarchical procedure. The hierarchical scheme is an iterative method which starts with a collection of $N_p = 2^p$ particles at iteration $i = 0$ and ends with a unique aggregate of N_p particles at iteration p. At an intermediate iteration i, one has a collection of $N_c = 2^{p-i}$ independent aggregates, each of them containing $N = 2^i$ particles. To proceed to the next iteration, the 2^{p-i} aggregates are grouped into pairs and a new aggregate is built with each pair according to a specific sticking rule. As soon as it is obtained, the new aggregate is randomly disoriented and is stored in the collection for the next iteration. The sticking rules depend on the chosen aggregation process. In the CLCA case the sticking rule is as follows: A particle of one cluster and a particle of another cluster are chosen at random as well as a random direction in space. The two clusters are disposed such that these two particles are in contact with their centers aligned along a random direction. Then a test of overlap is made for the other particles. If an overlap is found, the trial is discarded and another choice is made for both particles and random direction. Then, the resulting aggregate is stored for the next iteration. In this model, the resulting fractal dimension[15] is equal to about 2.

In this work the hierarchical procedure is initialized with a collection of N polydisperse particles whose diameters a_i are distributed according to a truncated Gaussian distribution. We use a standard library subroutine which generates a set of random variables x_i of zero mean and standard deviation equal to one, distributed according to the normal probability law:

$$g(x) = \frac{1}{\sqrt{2\pi}} e^{-x^2/2}. \tag{1}$$

The diameters a_i are calculated by

$$a_i = 1 + s x_i, \tag{2}$$

where s is an input parameter and where all the x_i's leading to negative a_i's have been discarded. Then we calculate the average a_0 and the standard deviation σ from the usual formulas:

$$a_0 = \frac{1}{N} \sum_{i=1}^{N} a_i \tag{3a}$$

and

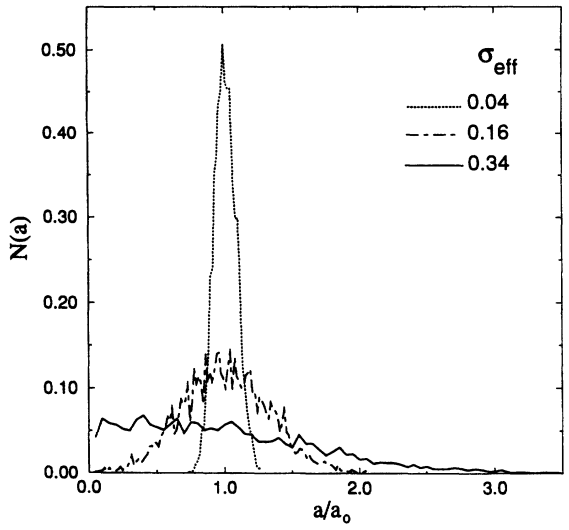

FIG. 1. Histograms of the particle size Gaussian-like distribution for three different σ_{eff} values.

$$\sigma^2=\frac{1}{N}\sum_{i=1}^{N}(a_i-a_0)^2. \tag{3b}$$

By varying the parameter s, one can vary the effective standard deviation $\sigma_{\text{eff}}(=\sigma/a_0)$, which is the only relevant dimensionless parameter in our problem. Note that σ_{eff} is practically equal to s for $s\leq 0.17$, where $a_0\simeq 1$. In Fig. 1 we show typical histograms for different values of σ_{eff}.

In the general case (where the standard deviation may be large) one can no longer calculate the scattered intensity $I(q)$ as a product of a form factor $P(q)$ and the structure factor $S(q)$. One should go back to the calculation of the scattered amplitude,[16] which is proportional to:

$$\tilde{A}=\sum_i \int_v e^{i\vec{q}\cdot(\vec{r}_i+\vec{x})}d^3x, \tag{4}$$

where $\vec{r}_i$ refers to the center of the ith particle and $\vec{x}$ refers to a running point inside the volume of the ith particle with respect to its center. The integral inside the sum, which should be performed over the volume of the ith particle, can be calculated as a function of a_i, assuming isotropy and homogeneity inside the sphere, leading to

$$\tilde{A}=\sum_i e^{i\vec{q}\cdot\vec{r}_i}A_i(q) \tag{5a}$$

with

$$A_i(q)=4\pi\frac{\sin\left(\frac{qa_i}{2}\right)-\left(\frac{qa_i}{2}\right)\cos\left(\frac{qa_i}{2}\right)}{q^3}. \tag{5b}$$

Then, assuming a random orientation of the aggregate over the direction of $\vec{q}$, the scattered intensity $I(q)=|\tilde{A}|^2$ can be written as

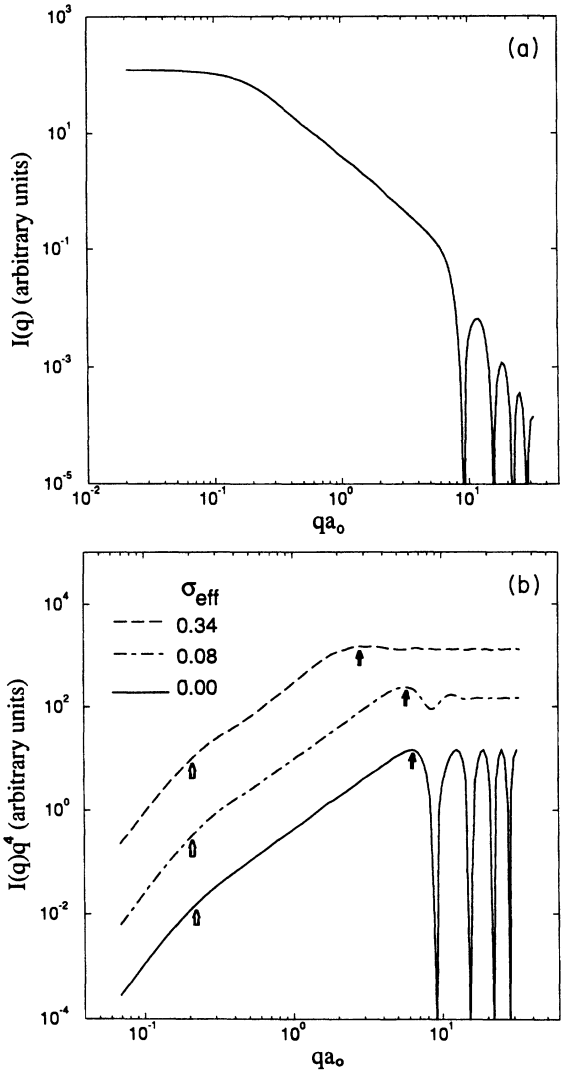

FIG. 2. (a) Log-log plot of $I(q)$ versus qa_0 for $\sigma_{\text{eff}}=0$. (b) Log-log plot of $I(q)q^4$ versus qa_0 for three different σ_{eff} values. The white arrows indicate the crossover between the Guinier and the fractal regime. The black arrows indicate the crossover between the fractal and the Porod regime. All these curves result from an average over 32 simulations with $N=128$ particles.

$$I(q)=\sum_{i,j}A_iA_j\frac{\sin(qr_{ij})}{qr_{ij}}, \tag{6}$$

where $r_{ij}=|\vec{r}_i-\vec{r}_j|$.

Note that, since the i and j dependent product A_iA_j appears inside the sum, the result cannot be split in two parts. In particular one cannot use the distance distribution function $f(r)=\Sigma_{i,j}\delta(r-r_{ij})$ to calculate an intermediate structure factor $S(q)$. Here the double sum has been calculated directly.

The numerical results are reported in Fig. 2 where we have plotted the intensity $I(q)$ as a function of the "reduced" wave vector qa_0. In Fig. 2(a) is shown the $I(q)$ curve obtained for $\sigma_{\text{eff}}=0$; in this curve we can observe the three regimes mentioned above. Figure 2(b) shows three $I(q)$ curves corresponding to three aggregates of different σ_{eff} values. In this figure, in order to better see the crossover

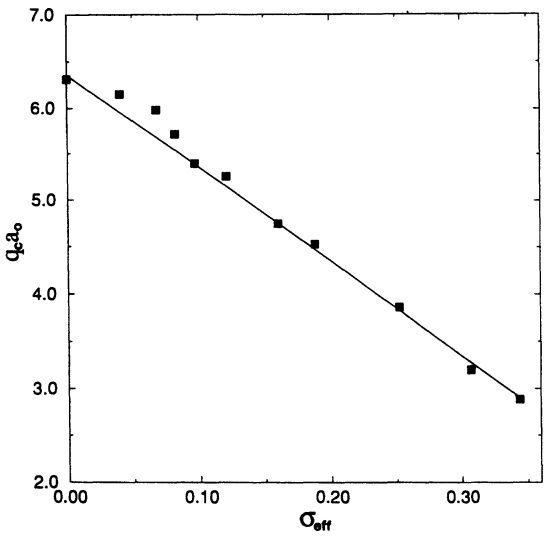

FIG. 3. Plot of $q_c a_0$ versus σ_{eff}.

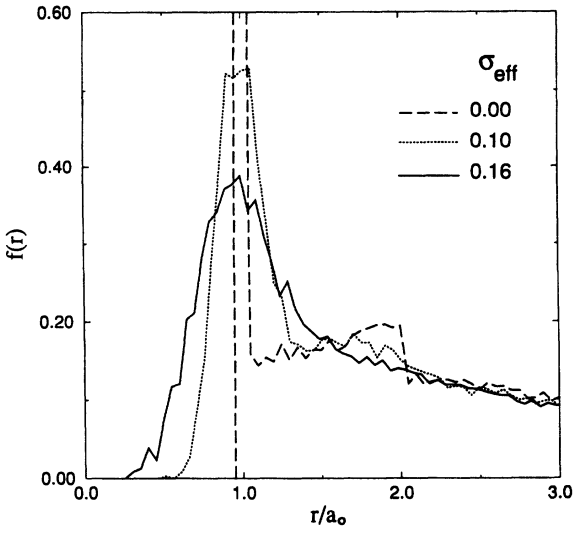

FIG. 4. Plots of $f(r)$ versus r for three σ_{eff} values. All these curves result from an average over 32 simulations with $N=128$ particles.

between the fractal and the Porod regime, we use the convenient $I(q)q^4$ representation where the first maximum corresponds to the crossover. As indicated by the arrows on the left of Fig. 2(b), the location of the crossover between the Guinier and the fractal regime is the same in all cases. Also, the slope of the fractal regime is unchanged. These two results mean that the particle size polydispersity does not affect the intra-aggregate long-range particle correlations as well as the overall size of the aggregate. However, the location of the maximum corresponding to the crossover between the fractal and the Porod regime strongly depends on σ_{eff}. In the monodisperse case ($\sigma_{\text{eff}}=0$), one has $q_c a_0=2\pi$, as expected, but, for increasing σ_{eff} values, $q_c a_0$ is pushed towards low values. On the other hand, in Fig. 2(b), one observes how the oscillations of the Porod regime are more and more damped as the degree of polydispersity increases.

In Fig. 3 we report the variation of $q_c a_0$ as a function of σ_{eff}. There is first a quite slow decrease, but after a sigmoidal-like behavior, $q_c a_0$ reaches, for $\sigma_{\text{eff}}>0.1$, a net linear behavior which can be approximated by

$$q_c=\frac{2\pi}{a_0}(1-1.6\sigma_{\text{eff}}). \tag{7}$$

The overall decrease of $q_c a_0$ when increasing polydispersity can be attributed to the fact that larger particles dominate the scattering.

In order to understand the small change of regime observed near $\sigma_{\text{eff}}=0.1$ in Fig. 3, we have calculated the center-to-center interparticle distribution function $f(r)$ for aggregates of different degrees of polydispersity, which has been normalized as follows:

$$\int_0^\infty f(r)4\pi r^2 dr=\frac{N-1}{2}, \tag{8}$$

where N is the number of particles of the aggregate.

In practice, to calculate $f(r)$, we choose a given path δr, and we calculate the number of interparticle distances lying between r and $r+\delta r$. Then we divide the result by $4\pi r^2 N\delta r$. In Fig. 4 we compare $f(r)$ curves with $\sigma_{\text{eff}}=0.1$ and with $\sigma_{\text{eff}}=0.16$ with the monodisperse curve ($\sigma_{\text{eff}}=0$). The δ peak at $r/a_0=1$ as well as the discontinuity at $r/a_0=2$, which has been attributed to short-range interparticle correlations in a previous publication,[11] are progressively washed out when introducing polydispersity. Even if $I(q)$ and $f(r)$ are not directly related, it is worth noticing that the bump observed in Fig. 3 occurs at the value $\sigma_{\text{eff}}=0.1$ at which the two peaks merge into a single broad peak. Therefore the change of behavior occurring near $\sigma_{\text{eff}}=0.1$ can be attributed to a modification of the short-range correlations due to polydispersity. Note that such effects have nothing to do with the truncation of the Gaussian distribution that we have considered since this truncation be-

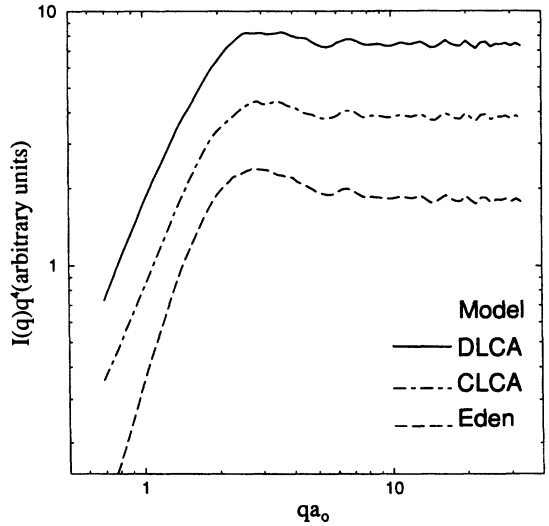

FIG. 5. Log-log plots of $I(q)q^4$ versus qa_0 for three different models with $\sigma_{\text{eff}}=0.34$. All these curves result from an average over 32 simulations with $N=128$ particles.

comes effective for $\sigma_{\text{eff}} > 0.17$. On the other hand, we can understand why the $I(q)$ curve presents only one maximum at high-q for $\sigma_{\text{eff}} > 0.1$ [see Fig. 2(b)].

We have considered other aggregation models: the diffusion-limited cluster-cluster aggregation[17,18] (DLCA) and chemically limited particle-cluster aggregation (the so-called Eden model[19]). The first model gives a fractal aggregate with a fractal dimension $D \simeq 1.78$, and the second model corresponds to a homogeneous aggregate of dimension equal to 3. In Fig. 5 we show the two $I(q)$ resulting curves for a fixed value of σ_{eff}, in comparison with the CLCA case. In this Fig. 5, we see that the crossover between the fractal regime and Porod regime remains at the same $q_c a_0$ value. This fact is due to the common short-range correlations in all the considered cases, meaning that relation (7) is valid for a wide range of aggregated systems.

In summary, we have demonstrated that the crossover between the fractal regime and the Porod regime is very sensitive to the particle polydispersity. An empirical relation between the crossover wave vector q_c, the particle average diameter a_0, and the standard deviation σ was obtained. We have also shown that the results are almost independent on the aggregation mechanism.

We acknowledge interesting discussions with M. Foret. One of us (A.H.) would like to acknowledge support from CONICIT (Venezuela). Laboratoire de Science des Matériaux Vitreux is Unité Associée au CNRS No. 1119.

[1] S. H. Chen and J. Teixeira, Phys. Rev. Lett. **57**, 2583 (1986).

[2] T. Freltoft, J. K. Kjems, and S. K. Sinha, Phys Rev. B **33**, 269 (1986).

[3] G. Dietler, C. Aubert, and D. S. Cannell, Phys. Rev. Lett. **57**, 3117 (1986).

[4] R. Vacher, T. Woigner, J. Pelous, and E. Courtens, Phys. Rev. B **37**, 6500 (1988).

[5] D. W. Schaefer and K. D. Keefer, Phys. Rev. Lett. **56**, 2199 (1986).

[6] A. Boukenter, D. Champagnon, J. Dumas, E. Duval, J. F. Quinson, J. L. Rousset, J. Serughetti, S. Etienne, and C. Mai, Rev. Phys. Appl. (Paris) **24**, C4-133 (1989).

[7] F. Chaput, A. Lecomte, A. Dauger, and J. P. Boilot, Rev. Phys. Appl. (Paris) **24**, C4-137 (1989).

[8] D. Posselt, J. S. Pedersen, and K. Mortensen, J. Non-Cryst. Solids **145**, 128 (1992).

[9] A. Guinier and J. Fournet, *Small Angle Scattering of X-rays* (Wiley Interscience, New York, 1955).

[10] A. Hasmy, E. Anglaret, M. Foret, J. Pelous, and R. Jullien, Phys. Rev. B (to be published).

[11] A. Hasmy, M. Foret, J. Pelous, and R. Jullien, Phys. Rev. B **48**, 9345 (1993).

[12] R. Jullien and R. Botet, *Aggregation and Fractal Aggregates* (World Scientific, Singapore, 1987).

[13] R. Botet, R. Jullien, and M. Kolb, J. Phys. A **17**, L75 (1983).

[14] R. Jullien and M. Kolb, J. Phys. A **17**, L639 (1984).

[15] B. B. Mandelbrot, *Fractals: Form Chance, and Dimension* (Freeman, San Francisco, 1977).

[16] L. A. Feigin and P. I. Svergun, *Structure Analysis by Small Angle X-rays and Neutron Scattering* (Plenum, New York and London, 1987).

[17] P. Meakin, Phys. Rev. Lett. **51**, 1119 (1983).

[18] M. Kolb, R. Botet, and R. Jullien, Phys. Rev. Lett. **51**, 1123 (1983).

[19] M. Eden, *Proc. 4th Berkeley Symp. Math. Stat. Prob.* (University of California Press, Berkeley, 1961), Vol. 4, p. 223.